An intrinsically three dimensional fractal

M. Fernández Guasti

March 18, 2013

Lab. de Óptica Cuántica, Depto. de Física,
Universidad A. Metropolitana - Iztapalapa,
09340 México D.F., Ap. postal. 55-534, MEXICO
e-mail: mfg@xanum.uam.mx, url: http://luz.izt.uam.mx

Abstract

The quadratic iteration is mapped using a non distributive real scator algebra in three dimensions. The bound set has a rich fractal like boundary. However, the two dimensional (1+1) projection becomes identical to the quadratic iteration produced with hyperbolic numbers. The quadratic iteration with hyperbolic numbers does not produce a fractal structure.

The hyperbolic numbers square bound set reveals a rich structure when taken into the three dimensional hyperbolic scator space. Self similar small copies of the larger set are obtained along the real axis. Furthermore, these small copies are self similar 3D copies of the larger 3D bound set. The real roots of the respective polynomials exhibit basins of attraction in a three dimensional space. Slices of the 3D confined scator set, labeled $\mathbf{c2i0}\mathbb{E}^2(s;x,y)$, are shown at different planes to give an approximate idea of the 3D object highly complicated boundary.

Keywords: Fractals; Hyper-complex numbers; 3D hyperbolic numbers; Real scators; Quadratic iteration; Mandelbrot set.

1 Introduction

Two dimensional fractal structures have often been extended to higher dimensions. For example: Sierpinski triangles are extended to three dimensional tetrahedrons that produce square based pyramids; Sphere inversion fractals as a generalization of circle inversion [**?**]; Mandelbrot, Mandelbox and several other approaches to generalizations of fractals in the complex plane to three dimensions, etc. However, the generalization does not always produce a three dimensional fractal structure. For example, quaternion quadratic iterations in parameter space produce solids of revolution with an M-set section.

On the other hand, it is not common practice to proceed the other way around. Namely, to produce a three dimensional fractal structure and thereafter to obtain two dimensional projections of these objects. Nonetheless, it will be the procedure followed here. Namely, we will propose an algebra that produces a three dimensional fractal structure. The product in this scator algebra is not distributive over addition. Furthermore, not all elements are invertible and the product is associative only if divisors of zero are excluded.

It thus comes as a surprise that a two dimensional non fractal structure is generalized to a three dimensional fractal structure.

2 Hyperbolic scators

Real scator elements in 1+2 dimensions can be written in terms of three real numbers

$$\overset{o}{\varphi} = (F_0; F_1, F_2)\,,\ F_j \in \mathbb{R}.$$

The first component stands on a different footing from the rest. To stress this fact, it is separated by a semi-colon from the other components. It is labeled with subindex zero and named the scalar component. Subsequent components, separated by commas, stand on an equal footing. They are named the director components because, as we shall see, they possess a direction. Scator elements are represented with an oval placed overhead[1]. The *addition* operation for scators $\overset{o}{\alpha}, \overset{o}{\beta}$ is defined component-wise

$$\overset{o}{\alpha} + \overset{o}{\beta} \equiv (A_0; A_1, A_2) + (B_0; B_1, B_2) = (A_0 + B_0; A_1 + B_1, A_2 + B_2)\,.$$

The scator set forms a commutative group under the addition operation. The *product* operation for scators, $\overset{o}{\alpha} = (A_0; A_1, A_2)$ and $\overset{o}{\beta} = (B_0; B_1, B_2)$ is defined by $\overset{o}{\gamma} = \overset{o}{\alpha}\overset{o}{\beta} = (G_0; G_1, G_2)$, where the scalar component of the product is

$$G_0 = A_0B_0 + A_1B_1 + A_2B_2 + \frac{A_1B_1A_2B_2}{A_0B_0} \tag{2.1a}$$

and the director components of the product are

$$G_1 = B_0A_1 + A_0B_1 + \frac{A_1A_2B_2}{A_0} + \frac{A_2B_1B_2}{B_0}, \tag{2.1b}$$

[1] \overset{o} in LaTeX lore

$$G_2 = B_0 A_2 + A_0 B_2 + \frac{A_1 A_2 B_1}{A_0} + \frac{A_1 B_1 B_2}{B_0}. \tag{2.1c}$$

In order to have a well defined product, it is necessary that the scalar components are different from zero if two or more director components are different from zero. The subspace space $\mathbb{E}^2 \subseteq \mathbb{R}^3$, where the product is well defined is

$$\left(\mathbb{E}^2, \cdot\right) = \left\{ \overset{o}{\alpha}, \overset{o}{\beta} \in \mathbb{E}^2 : A_0, B_0 \neq 0 \text{ if } A_1 B_1, A_2 B_2 \neq 0 \right\}. \tag{2.2}$$

Hyperbolic 1+2 dimensional scators form a commutative group under the product operation provided that non invertible elements and divisors of zero are excluded. The subspace $\mathbb{E}_g^2$ where the product forms a commutative group is

$$\left(\mathbb{E}_g^2, \cdot\right) = \left\{ \overset{o}{\alpha}, \overset{o}{\beta} \in \left(\mathbb{E}^2, \cdot\right) : \overset{o}{\alpha}, \overset{o}{\beta} \neq 0, A_0 \neq A_k, B_0 \neq B_k, \frac{A_k B_k}{A_0 B_0} \neq -1, k = 1, 2 \right\}. \tag{2.3}$$

The square of a scator is obtained from the product definition (2.1a)-(2.1c) between two equal scators $\overset{o}{\beta} = \overset{o}{\alpha}$. Let $A_0 = B_0 = s$, $A_1 = B_1 = x$ and $A_2 = B_2 = y$. The square of the scator $\overset{o}{\alpha} = (s; x, y)$ is then $\overset{o}{\gamma} = \overset{o}{\alpha}^2 = (G_0; G_1, G_2)$ with

$$G_0 = s^2 + x^2 + y^2 + \frac{x^2 y^2}{s^2} \tag{2.4a}$$

and the director components of the product are

$$G_1 = 2sx + \frac{2xy^2}{s} = 2x \left(s + \frac{y^2}{s} \right) \tag{2.4b}$$

$$G_2 = 2sy + \frac{2yx^2}{s} = 2y \left(s + \frac{x^2}{s} \right). \tag{2.4c}$$

The square of the magnitude of a scator $\left\| \overset{o}{\varphi} \right\|^2$ for a scator $\overset{o}{\varphi} = (F_0; F_1, F_2)$ is defined by

$$\left\| \overset{o}{\varphi} \right\|^2 = \overset{o}{\varphi} \overset{o}{\varphi}{}^* = \left(F_0^2 - F_1^2 - F_2^2 + \frac{F_1^2 F_2^2}{F_0^2}; 0, 0 \right). \tag{2.5}$$

The subspace $\mathbb{E}^2$ where the product is well defined, from (2.2), requires that $s \neq 0$ if $x \neq 0$ and $y \neq 0$. If s becomes very small while x, y are finite, the magnitude of the scator becomes very large. Therefore, no points will be bound in the plane x, y in the vicinity of $s = 0$. Repelling points on the plane.

The only points within the x, y plane that can be (but are not necessarily) confined for $s = 0$ are the lines for $x = 0$ or $y = 0$. If $x = 0$, $\overset{o}{\alpha} = (s; 0, y)$

$$\overset{o}{\gamma} = \overset{o}{\alpha}^2 = \left(s^2 + y^2; 0, 2sy\right)$$

and the iteration is

$$\overset{o}{\varphi}_2 = \overset{o}{\alpha}^2 + \overset{o}{\alpha} = \left(s^2 + y^2 + s; 0, 2sy + y\right)$$

The limit when $s \to 0$, can now be taken and gives

$$\overset{o}{\gamma} = \left(y^2; 0, 0\right)$$

this has to be discussed in iteration: furthermore, iterations

$$\begin{aligned}
\overset{o}{\varphi}_0 &= (0; 0, 0) \\
\overset{o}{\varphi}_1 &= (0; 0, y) \\
\overset{o}{\varphi}_2 &= \left(y^2; 0, y\right) \\
\overset{o}{\varphi}_3 &= \left(y^4 + y^2; 0, 2y^3 + y\right) \\
\overset{o}{\varphi}_4 &= \left(\left(y^4 + y^2\right)^2 + \left(2y^3 + y\right)^2; 0, 2\left(y^4 + y^2\right)\left(2y^3 + y\right) + y\right) \\
&\vdots
\end{aligned}$$

and the scator magnitudes for each iteration are

$$\begin{aligned}
\left\|\overset{o}{\varphi}_0\right\| &= (0; 0, 0) \\
\left\|\overset{o}{\varphi}_1\right\| &= \left(y^2; 0, 0\right) \\
\left\|\overset{o}{\varphi}_2\right\| &= \left(y^4 - y^2; 0, 0\right) \\
\left\|\overset{o}{\varphi}_3\right\| &= \left(\left(y^4 + y^2\right)^2 - \left(2y^3 + y\right)^2; 0, 0\right) \\
\left\|\overset{o}{\varphi}_4\right\| &= \left(\left(\left(y^4 + y^2\right)^2 + \left(2y^3 + y\right)^2\right)^2 - \left(2\left(y^4 + y^2\right)\left(2y^3 + y\right) + y\right)^2; 0, 0\right) \\
&\vdots
\end{aligned}$$

If the magnitudes of the scalar part $\mathcal{S}c\left\{\overset{o}{\varphi}\right\} = \frac{1}{2}\left(\overset{o}{\varphi} + \overset{o}{\varphi}^*\right)$, are considered separately, $\left\|\mathcal{S}\left\{\overset{o}{\varphi}\right\}\right\|^2 = \frac{1}{4}\left(\overset{o}{\varphi} + \overset{o}{\varphi}^*\right)^2 = \left(F_0^2; 0, 0\right)$, the scalar magnitudes for each iteration are

$$
\begin{aligned}
\left\| \mathcal{S}\left\{ \overset{o}{\varphi}_0 \right\} \right\| &= (0;0,0) \\
\left\| \mathcal{S}\left\{ \overset{o}{\varphi}_1 \right\} \right\| &= \left(y^2;0,0\right) \\
\left\| \mathcal{S}\left\{ \overset{o}{\varphi}_2 \right\} \right\| &= \left(y^4;0,0\right) \\
\left\| \mathcal{S}\left\{ \overset{o}{\varphi}_3 \right\} \right\| &= \left(\left(y^4+y^2\right)^2;0,0\right) \\
\left\| \mathcal{S}\left\{ \overset{o}{\varphi}_4 \right\} \right\| &= \left(\left(\left(y^4+y^2\right)^2+\left(2y^3+y\right)^2\right)^2;0,0\right) \\
&\vdots
\end{aligned}
$$

The set should be confined by the vertical line at the origin of the square of the hyperbolic case. Since the square is rotated $\pi/4$, ant the tip from the origin on the RHS is located at $\frac{1}{4}$. Then, the bound limit should be located at $y=\frac{1}{4}$ if magnitudes are evaluated separately .

$$
\overset{o}{\varphi}_{n+1} = \overset{o}{\varphi}{}_n^2 + \overset{o}{c},
$$

with $\overset{o}{c} = (c_s;0,c_y)$; in this case $\overset{o}{c} = (0;0,c_y)$

$$
(s_{n+1};0,y_{n+1}) = \left(s_n^2+y_n^2;0,2s_ny_n+c_y\right),
$$

and for the scalar part

$$
s_{n+1} = s_n^2 + y_n^2
$$

for the director part

$$
y_{n+1} = 2s_ny_n + c_y
$$

test for scalar part:

$$
s_{n+1} - s_n = s_n^2 - s_n + y_n^2
$$

the function w^2-w has a minimum at $2w-1=0$, that is at $\frac{1}{2}$ and the value at the minimum is $\left(\frac{1}{2}\right)^2 - \frac{1}{2} = -\frac{1}{4}$. Therefore $s_n^2 - s_n \geq -\frac{1}{4}$.

If we were in the reals and the constant had a term c_s, then $y_n = 0$ and $s_{n+1}-s_n = s_n^2 - s_n + c_s$. The value $c_s = \frac{1}{4}+\varepsilon$ gives $s_{n+1}-s_n = s_n^2 - s_n + c_s \geq -\frac{1}{4}+\frac{1}{4}+\varepsilon$, thus $s_{n+1} > s_n$, the terms increase and the iteration diverges.

test for director part:

$$
y_{n+1} - y_n = (2s_n - 1)\, y_n + c_y
$$

evaluate

$y_{n+2} = 2s_{n+1}y_{n+1}+c_y = 2s_{n+1}\left(2s_ny_n + c_y\right)+c_y = 2\left(s_n^2 + y_n^2\right)\left(2s_ny_n + c_y\right)+c_y$

then from $y_{n+1} = 2s_ny_n + c_y$,

$$\frac{y_{n+1} - c_y}{2y_n} = s_n$$

and if we substitute in

$$y_{n+2} = 2\left(s_n^2 + y_n^2\right)\left(2s_ny_n + c_y\right) + c_y$$

we obtain

$$y_{n+2} = 2\left(\left(\frac{y_{n+1} - c_y}{2y_n}\right)^2 + y_n^2\right)\left(2\frac{y_{n+1} - c_y}{2y_n}y_n + c_y\right) + c_y$$

$$y_{n+2} = 2\left(\left(\frac{y_{n+1} - c_y}{2y_n}\right)^2 + y_n^2\right)(y_{n+1}) + c_y$$

$$y_{n+2} = 2\left(\left(\frac{y_{n+1}^2 + c_y^2 - 2c_yy_{n+1}}{4y_n^2}\right) + y_n^2\right)(y_{n+1}) + c_y$$

$$2y_{n+2}y_n^2 = \left(y_{n+1}^2 + c_y^2 - 2c_yy_{n+1} + 4y_n^4\right)(y_{n+1}) + 2y_n^2c_y$$

$$2y_{n+2}y_n^2 = y_{n+1}^3 + c_y^2y_{n+1} - 2c_yy_{n+1}^2 + 4y_n^4y_{n+1} + 2y_n^2c_y$$

...

Divisors of zero for non invertible elements are obtained if the equalities $A_1B_1 = -A_0B_0$ and $A_2B_2 = -A_0B_0$ are fulfilled. For the quadratic mapping, these conditions are never met, since for two identical scators, they imply that $x^2 = -s^2$ and $y^2 = -s^2$. However, since s, x, y are real, the condition is never attained. There are therefore no nilpotent elements in real scator algebra under the quadratic iteration.

On the other hand, consider an invertible element, that is, an element where $s \neq x$ and $s \neq y$ and $y \neq 0$. The square of this element is also an invertible element since G_0 in (2.4a) is always different from zero.

The only non associative elements come from non invertible elements with $x^2 = s^2$ or $y^2 = s^2$.

Notice that the special relativity metric is recovered for $F_0^2 \gg F_1^2, F_2^2$ if the scalar component is identified with time and the director components with two spatial axes. On these grounds, an alternative composition of velocities in a deformed Lorentz metric has been proposed using real scator algebra [8]. If condition (2.3) is fulfilled, the scator product of the norm is equal to the norm of the scator products. This identity permits a generalization of Lagrange's identity. Furthermore, the scator norm product identity produces an infinite number of series identities [9].

3 Iterated quadratic mapping

The quadratic mapping is given by

$$\overset{o}{\varphi} = \overset{o}{\varphi}_0^2 + \overset{o}{c},$$

where the variable $\overset{o}{\varphi}$ and the constant $\overset{o}{c}$ are now scator elements. The iterated function satisfies the recurrence relationship

$$\overset{o}{\varphi}_{n+1} = \overset{o}{\varphi}_n^2 + \overset{o}{c},$$

where the subindex stands for the iteration number. The Mandelbrot like set is obtained by fixing the initial point $\overset{o}{\varphi}_0 = (0;0,0)$ and varying the parameter $\overset{o}{c}$. Bounded points obtained with this procedure comprise the corresponding M-set in $\mathbb{E}^2$. There is an arbitrary number of intersections of the plane with a volume depending on the position and inclination of the plane. Therefore, there are infinitely many slices of the M-like set in $\mathbb{E}^2$ compared with the unique set obtained in $\mathbb{C}$. The following notation will be used to allow for some orientation in several dimensions

- **c2i** confined {**2**}quadratic iterations, (can be generalized to **cpi** for a p$^{\text{th}}$ power polynomial or p$\rightarrow$ *func* for other *func*tion's mappings)
- followed by **0** if the initial value of the variable is set to zero as it happens in parameter space
- followed by the number set: $\mathbb{R}$ real, $\mathbb{C}$ complex, $\mathbb{H}$ hyperbolic, $\mathbb{E}^n$ real scator (in 1+n dimensions), etc.
- followed, if required, by the plane $(D_0; D_1, D_2)$ that is being depicted.

According to this notation, the Mandelbrot set in the complex plane is labeled as the **c2i0**$\mathbb{C}$ set. It is not necessary to show explicitly the plane that is being depicted since it is inevitably the complex plane.

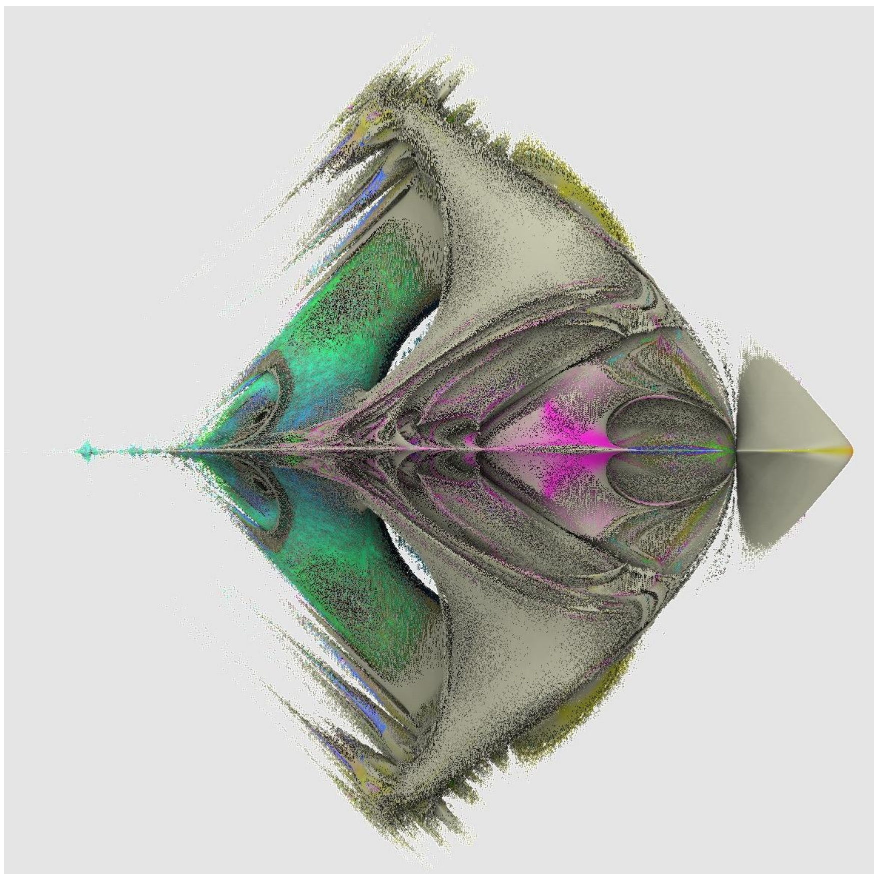

Figure 1: Image of a three dimensional rendering of the $\mathbf{c2i0}\mathbb{E}^2(s; x, y)$ set viewed from the second director component y axis. The abscissa corresponds to the real or scalar s axis while the ordinate corresponds to the first director component x axis. 12 iterations were used $-2.14 < s < 0.62$, $-1.42 < x < 1.34$, $-0.97 < y < 1.79$,

The M-like set for real scators in 1+2 dimensions, according with the proposed notation, is written as the $\mathbf{c2i0}\mathbb{E}^2$ set. This $\mathbf{c2i0}\mathbb{E}^2$ set is no longer in two dimensions but in a three dimensional space. In figure 1, a three dimensional rendering is shown. This and subsequent three dimensional images were produced with P. Willenius rendering program [11, v.2.0.1]. The colouring is due to the value of $(s$ (red); x (green), y (blue)) in the last iteration $(s_{12}$ (red); x_{12} (green), y_{12} (blue)).

On the other hand, distributivity of the product over addition does not hold. Consider the second iteration in terms of the initial value

$$\overset{o}{\varphi}_2 = \overset{o}{\varphi}{}_1^2 + \overset{o}{c} = \left(\overset{o}{\varphi}{}_1^2 + \overset{o}{c}\right)^2 + \overset{o}{c} = \left(\overset{o}{\varphi}{}_1^2 + \overset{o}{c}\right)\left(\overset{o}{\varphi}{}_1^2 + \overset{o}{c}\right) + \overset{o}{c}. \tag{3.1}$$

This scator is not equal to $\overset{o}{\varphi}{}_2' = \overset{o}{\varphi}{}_1^4 + 2\overset{o}{c}\,\overset{o}{\varphi}{}_1^2 + \overset{o}{c}{}^2 + \overset{o}{c}$. The numerical procedure evaluates the scator in each iteration and then proceeds to the next. Therefore, it produces sequences of the form described by equation (3.1). Notice that for hyperbolic numbers or scators with a single director component distributivity holds, $\overset{o}{\varphi}_2\ (s;0,y) = \overset{o}{\varphi}{}_2'\ (s;0,y)$ and either expression yields the same results.

Let us return to figure **??**; It is symmetrical with respect to the hypercomplex ordinate axis $\hat{\mathbf{e}}_x$. Let us confirm that this is the expected result. The first two iterations starting with $\overset{o}{\varphi}_0 = (0;0,0)$ are $\overset{o}{\varphi}_1 = \overset{o}{c}$ and $\overset{o}{\varphi}_2 = \overset{o}{c}{}^2 + \overset{o}{c}$. The scator number squared plus the scator is

$$\overset{o}{\varphi}_2 = (s_2; x_2, y_2) = \overset{o}{\varphi}{}_1^2 + \overset{o}{\varphi}_1 = \\ \left(s^2 + x^2 + y^2 + \frac{x^2y^2}{s^2} + s;\ 2sx + \frac{2xy^2}{s} + x,\ 2sy + \frac{2yx^2}{s} + y\right). \tag{3.2}$$

The resulting $\hat{\mathbf{e}}_x$ director component is $2sx + \frac{2xy^2}{s} + x$. This expression is an odd function of x, thus upon iteration, the function will be equal but with opposite sign under the transformation $x \to -x$. The bound criterion to establish the confined set is the squared magnitude $\left\|\overset{o}{\varphi}\right\|^2 = \left(s^2 - x^2 - y^2 + \frac{x^2y^2}{s^2}; 0, 0\right)$. This function is even under inversion of any of the axes. Therefore, the confined set, or the escape velocity iso-surfaces must be symmetric about the $\hat{\mathbf{e}}_x$ ordinate axis. An equivalent reasoning leads to symmetry about the $\hat{\mathbf{e}}_y$ axis. On the other hand, the bound set is asymmetrical with respect to the scalar (or real) s axis. Indeed, from the above expression, the transformation $s \to -s$ does not have a well defined parity for the resultant scalar term $s^2 + x^2 + y^2 + \frac{x^2y^2}{s^2} + s$. Thus, the iterated map will not be equal under inversion of the scalar axis.

The bound set in figure **??** has an inner square on the right with a roundish centre. Let us analyze this feature. If the scalar becomes small, all three components in iteration (3.2) become large for nonzero director components. Allow for y to be negligible in the scalar term second iteration; Impose the condition $s_2 \to 0$, so that the scalar term will produce a very large scator on the third iteration, $s^2 + x^2 + s = 0$. Notice that the s terms can be collected as

$s^2+s=\left(s+\frac{1}{2}\right)^2-\frac{1}{4}$. The equation is then $\left(s+\frac{1}{2}\right)^2+x^2=\frac{1}{4}$, that is a circle of radius $\frac{1}{2}$ centered at $\left(-\frac{1}{2};0,0\right)$. Therefore, the roundish rim feature where the set is unbounded is due to the scalar component becoming very small. It is of course not strictly a circle because the non-zero second director term has been neglected. This shape is distorted as the y plane is further away from the origin as can be seen in figure 6. The roundish centre has two asymmetric triangular arrows on its sides. The point where the arrow on the right is joined to the main body is $s=0$. The tip of this arrow is located at $s=\frac{1}{4}$ as expected from the real axis bound interval $\left[-2,\frac{1}{4}\right]$. The arrow on the left is in fact a sequence of smaller copies of the main body, a feature that is observed when the iteration limit is increased. The upper and lower symmetric structures blend with a ragged bound region inscribed in a larger square. The ragged boundary seems to split into a Fatou dust-like fractal. The scale has been maintained equal to that of figure 8 to show that the escape velocity contours remain fairly similar in either case. The coordinates s and x are scanned from -2.2 to 2.2 in both figures.

In 1+1 dimensions, real scator algebra becomes identical to hyperbolic numbers algebra as may be readily seen from the product definition with any of the two director components with subindex 1 or 2 equal to zero. If we label the axes $(F_0;F_1,F_2)$ by s, $\hat{\mathbf{e}}_1$ and $\hat{\mathbf{e}}_2$, either plane $s,\hat{\mathbf{e}}_1$ or $s,\hat{\mathbf{e}}_2$ is identical to the hyperbolic number's plane.

Thus, the filled in Julia set in the complex plane K_c for the point $z=a+ib$ is the $\mathbf{c2i}(a,b)\mathbb{C}$ set. The K_c set for hyperbolic numbers is $\mathbf{c2i}(a,b)\mathbb{H}$ set and the M-set is $\mathbf{c2i0}\mathbb{H}$ set. This latter set is depicted in figure 8. The confined set is a square with smooth boundary. However, the layout of the escape values outside the set is already indicative of a richer structure. Since hyperbolic numbers are equivalent to scators with only one director component $\mathbb{H}\to\mathbb{E}^1$, the sets $\mathbf{c2i0}\mathbb{H}$ and $\mathbf{c2i0}\mathbb{E}^1$ are equal.

3.1 self-similarity - small copies

Let us have a closer look at the negative real scalar axis of the $\mathbf{c2i0}\mathbb{E}^2\left(s;x,10^{-17}\right)$ set in figure 3. It reveals smaller copies of itself! The pattern of the escape velocities in the vicinity of the set is quite complex. It exhibits straight bands at 45° whenever there is a copy of the larger set. Simultaneously there are well defined curves that resemble arcs of circles or parabolae in the midst of rather complicated structures. In figure **??**, several small copies of the larger set are observed between -2 and -1.4. The copy centered at $-1.769\cdots$ is shown on a larger scale in figure 3a. The number of iterations was increased as smaller regions are magnified, in order to preserve a similar resolution in the observed patterns. Its structure is remarkably similar to that of figure **??**. It reproduces the roundish centre with symmetric arrows on its sides and the symmetric structures above and below merging with a shred bound region inscribed in a larger

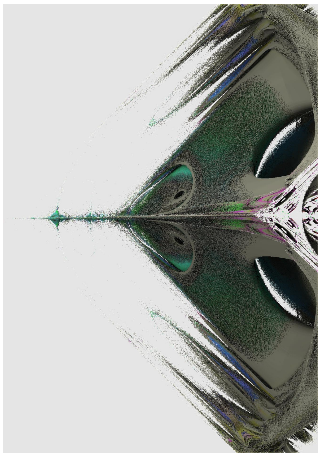

(a) inset of figure 1 with magnification $\times$ 2.2 limited to 12 iterations.$-2.1786 < s < -0.9482$, $-0.6560 < x < 0.5743$, $-0.1201 < y < 1.110$,

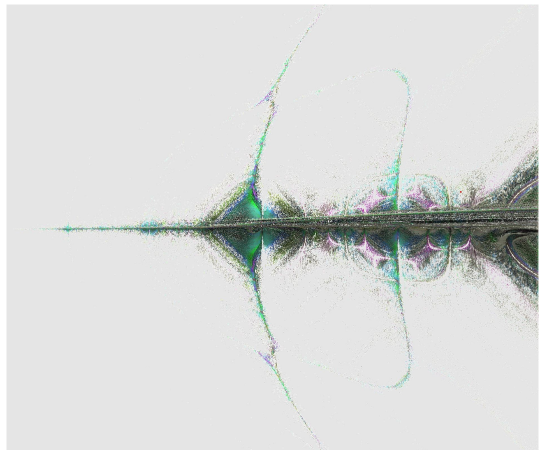

(b) inset of figure 1 with magnification $\times$ 11.3 limited to 12 iterations.$-1.8108 < s < -1.5678$, $-0.16238 < x < 0.08064$, $-0.97 < y < 1.79$,

Figure 2: Detail of the region located at -1.769 of the $\mathbf{c2i0}\mathbb{E}^2(s;x,y)$ set shown in figure **??**. Self-similar smaller copies of the diamond-like figure are observed!

square. It also exhibits even smaller copies of itself at a much smaller scale in between -1.792 and -1.7805.

This result is of course reminiscent of the self copies of the M-set in the complex plane $\mathbf{c2i0}\mathbb{C}$. The cardioïds situated between the Myrberg-Feigenbaum (MF) point $-1.401\ldots$ and -2 of the complex Mandelbrot set [10], are located at exactly the same positions on the real axis as the self- similar rhomboid-like figures of the $\mathbf{c2i0}\mathbb{E}^2(s;x,y)$ scator set within computer error. Furthermore, the relative size of the small cardioïd-like components are proportional to the relative size of the rhomboid-like figures. There are an infinite number of small copies of the larger M-set. The $\mathbf{c2i0}\mathbb{E}^2$ set seems to also have an equivalent infinite number of small copies of itself in the vicinity of the scalar axis. Just as the M-set has a period doubling cascade region converging towards the MF point, there are an infinite number of smaller diamond like figures in the scator set, apparently converging to this very same periodic-chaotic limit.

and

3.2 Planes with constant second director value

We have shown that a rich fractal like structure is revealed if the second director component is set to small value different from zero, (illustrated with

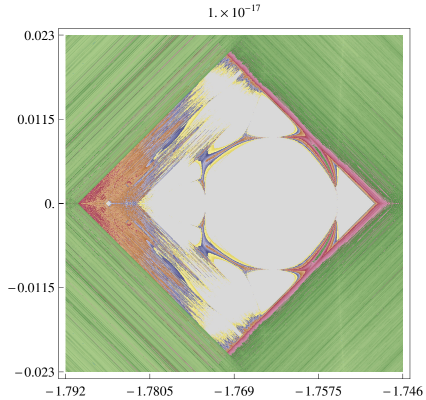

(a) inset of figure **??** with magnification $\times 95.6$ limited to 160 iterations.

Figure 3: Detail of the region located at -1.769 of the $\mathbf{c2i0}\mathbb{E}^2\left(s;x,10^{-17}\right)$ set shown in figure **??**. Self-similar smaller copies of the diamond-like figure are observed!

$y = 10^{-17}$). In figure 6, we show a sequence of sets from $\mathbf{c2i0}\mathbb{E}^2\left(s;x,10^{-20}\right)$ to $\mathbf{c2i0}\mathbb{E}^2\left(s;x,10^{-1}\right)$. Each point is evaluated starting with $\overset{o}{\varphi}_0 = (0;0,0)$ and $\overset{o}{c} = (s;x,y)$, s is scanned from -2.125 to 0.375, while x is scanned from -1.25 to 1.25. The bounded region becomes smaller and departs form the diamond-like shape moving steadily towards a bird-like form as y is increased. The imprint is always squeezed in the forefront to the right in a plane where $s = 0$. This result is expected because the scator magnitude (2.5) has a term $\frac{x^2y^2}{s^2}$ that diverges for non zero x, y. Thus, no scator iteration can be bound in the region where this term becomes very large. The wings have a central lobe and possibly a second smaller lobe. They become fuzzy on the edge where a Fatou dust like boundary is observed. The arrow on the left side becomes a tail with three protuberances. The upper and lower bulges resemble smaller copies of the wings. The protuberance on the left is a copy of the larger protuberance, most likely with doubling period just as the buds in this region in the complex Mandelbrot set. Eventually, at $y = 0.1$, the tail is almost detached from the main body.

In another sequence, depicted in figure 7, we show sets from $\mathbf{c2i0}\mathbb{E}^2(s;x,0)$ to $\mathbf{c2i0}\mathbb{E}^2(s;y,1.1)$ in steps of $\triangle y = 0.1$. Again, points are evaluated starting at $\overset{o}{\varphi}_0 = (0;0,0)$ and $\overset{o}{c} = (s;x,y)$, s is scanned in the ± 1.25 interval centered at $-\frac{7}{8} = -0.875$, while x is centered at 0. The first and second insets in figure 7 correspond to the initial and final insets in figure 6. The bound set becomes smaller as the distance from $y = 0$ increases. There are no longer visible bound points at $y = 0.2$ for positive s (The bird looses its head). At $y = 0.3$, the remnants of the left arrow vanish and the bound region lies within the $(-0.875, 0)$ interval (The bird looses its tail). The out-most bound point must be located at $y = \frac{9}{8} = 1.125$ where the upper tip of the diamond is located. Recall that there must be a diamond-like shape in the perpendicular $s, \hat{\mathbf{e}}_y$ plane identical to the one shown in the first $s, \hat{\mathbf{e}}_x$ inset. This feature is not visible in the last inset of figure 7 because the tip becomes very thin and is thus difficult to see at this magnification. Indeed, from the sequence in figure 6, it can be seen that the tip is approximately 10^{-7} thick between 1.0 and 1.125.

4 quadratic iteration with hyperbolic numbers

The quadratic iteration with hyperbolic numbers gives rise to a square centered at $-\frac{7}{8}$ with sides equal to $\frac{9}{4\sqrt{2}}$ [1]. Numeric evaluation of the quadratic iteration for initial $z_0 = 0$ The square diagonals (with $\frac{9}{4}$ length) lie parallel to the real and hypercomplex axes. If the bound criterion for a hyperbolic number $a + b\,\hat{\mathbf{e}}$, $(\hat{\mathbf{e}} \cdot \hat{\mathbf{e}} = 1,\ \hat{\mathbf{e}} \notin \mathbb{R})$ is $a^2 \leq \varepsilon$ and $b^2 \leq \varepsilon$, the bound set is equal to a square [2]. This set is the counterpart of the Mandelbrot set for complex numbers but in two dimensional hyperbolic geometry. The boundary for the hyperbolic set, is made up of four straight lines void of the complexity shown by the M-set. There are neither small-copies of the set nor a structure within the bound region as can be seen in figure 8.

The Julia sets obtained for arbitrary initial point z_0 give rise to rectangles [3]. These rectangles obtained for the hyperbolic case, are the twins of the filled in Julia sets K_c, for the quadratic iteration in the complex plane. It has been pointed out that if the bound criterion is established with the hyperbolic number magnitude $a^2 - b^2 \leq \varepsilon$, the confined set need not be rectangles [4]. Nonetheless, numeric evaluations using the hyperbolic number's magnitude $|z|^2 = a^2 - b^2$ still yield squares for the hyperbolic M-set and rectangular figures for the K_c sets. Panchelyuga et al. [5] have argued that this result is due to rounding errors introduced by the computing algorithms when dealing with the difference of very large numbers.

In this communication, we introduce a three dimensional hypercomplex algebra that contains the hyperbolic $\mathbb{H}$ numbers when only two components are considered. The hyperbolic or real scator algebra product is associative and commutative provided that divisors of zero are excluded. However, the product does not distribute over addition but in some special cases. It is possible to establish well defined rules for the quadratic mapping with real scator algebra. That is, the square and addition operations, although not bilinear, can be consistently constructed. Furthermore, an order parameter can be established so that a bound criterion can be employed. The bound set produced by scator numbers under the quadratic iteration mapping, exhibit small self-similar copies of the larger set. The boundary of the confined set has a rich structure. The contours of the iso-escape velocity sets also show rather elaborate patterns.

5 The x, y plane

Consider planes where the scalar component s is maintained constant, while the values in x, y are scanned. These plots are entirely new since both axes are now hypercomplex axes; There is no real axis in these plots! Confined sets should be obtained, at least in the vicinity of the origin, in the interval where s is between $\left[-2, \frac{1}{4}\right]$. In figure 9, $\mathbf{c2i0}\mathbb{E}^2(0.1; x, y)$ to $\mathbf{c2i0}\mathbb{E}^2(-1.1; x, y)$ sets are shown in steps of $\triangle s = 0.1$ for scans in x, y of ± 1. There are also confined sets images beyond $s = 1.1$ but with much smaller dimensions. The sets produced at x, y planes where self similar copies were observed in the s, x plane, also exhibit self similar structures in the x, y plane. Besides the inversion symmetry in the director components described in the previous section, there is symmetry when the two director components are interchanged in equation (3.2). Therefore, there is an additional 45° symmetry in the x, y plane as observed in the numerical results. The ek[2]-like figure depicted at $s = 0.1$ is repeated at various planes, for example from -0.6 to -0.9. The four turbans in the diagonals of inset at $s = -0.2$ alternate with diploid figures on the axes lines. At $s = -0.4$ straight lines with fuzzy edges come out producing a square shape. In the following insets remnants of the straight lines are displaced towards the edges until frame $s = -0.9$. At -1.0 an interlaced necklace can be seen with four droplets or tilab[3] at the ends. These tilab are made up of ever-smaller tilabs. There is a loltun[4] at the centre of the figure. The halo around the central confined figure is also a feature that reappears again and again, as may be seen in the last inset of figure 9.

6 Conclusions

The quadratic iteration in three dimensional real scator space exhibits a rich boundary structure with complex escape velocity surrounding patterns. The hyperbolic numbers square bound set is obtained when the real scator numbers are constrained to only two non vanishing components.

Self similar small copies of the larger bound set are obtained in the scalar (real) axis located at the same positions and relative sizes of the small M-set copies found on the real axis for the complex Mandelbrot set. Attractive fixed points are obtained when the quadratic function composition $R\left(R\left(R\left(z\right)\right)\right)\cdots = R^n\left(z\right)$ returns the original argument $R^n\left(z_0\right) = z_0$. In the real axis, they are obtained from the real roots of the polynomials $z = 0$, $z^2 + z = 0$, for a 1 period cycle; $\left(z^2 + z\right)^2 + z = 0$, for a 2 period cycle; $\left(\left(z^2 + z\right)^2 + z\right)^2 + z = 0$, for a 3 period cycle, etc. Recall that $\mathbb{R}$ is a subset of the $1 + m$ dimensional real scator set. Thus these roots, are also roots of the 1+2 dimensional scator set. It is

[2]ek-chaneb - star with four spikes in Mayan language.
[3]tilab - arrow in tseltal, one of the Mayan languages still spoken in southern Mexico.
[4]loltun - stone flower.

known that there are an infinite number of real polynomials' roots on this axis that come from the n^{th} cycle periods. Each of the fixed points has a basin of attraction. Furthermore, each of them exhibit self similar copies of the larger set. Hence, for the quadratic iteration with real scators, there are basins of attraction around the attractive fixed points in the scalar axis. These basins are observed in the s, x plane as shown in figure 3, the s, y plane (that is identical to the s, x plane) and the x, y plane as seen from figure 9. Thus, this real scator fractal set exhibits basins of attraction in a three dimensional space. Moreover, these small copies are self similar 3D copies of the larger 3D bound set.

Many questions open up regarding these new fractal structures. So far, we have found no evidence of self-similar structures lying outside the scalar axis. Whether they exist is an open problem. Little has been mentioned regarding the Julia sets produced with real scator numbers $\mathbf{c2i}(c_s; c_x, c_y)\,\mathbb{E}\,(s; x, y)$ and its relationship with the $\mathbf{c2i0}\mathbb{E}^2(s; x, y)$ set. This issue will be undertaken in a forthcoming communication. The $\mathbf{c2i0}\mathbb{E}^2(s; x, y)$ set is much more difficult to explore than the complex M-set since it involves a three dimensional structure. Two dimensional renderings can be made not only in planes with one constant component (as have been shown here) but also in inclined planes and even in non planar surfaces. Magnifications of different regions of the $\mathbf{c2i0}\mathbb{E}^2(s; x, y)$ set reveal extraordinary structures that we have only glimpsed at in an unsystematic fashion. 2D movies should prove useful to visualize the intricacies of the set [12]. Three dimensional renderings should also turn out to be very useful to visualize the nature of these confined quadratic iteration real scator sets. We have produced some preliminary images using a 3D rendering program [11] as the one reproduced in figure (10). The 3D self similar smaller set located around $(-1.75, 0, 0)$ is clearly visible. The two diamond shapes at the planes where one of the hypercomplex components is zero are also reckoned as well as the squezzing around the $s = 0$ plane on the far right. The various layers and the way they coalese are an ode to mathematical enchantment.

Acknowledgements

I am greatly indebted to Prof. A. Vilchis for his early critical reading of the scator algebra manuscripts.

References

[1] P. Senn. The Mandelbrot set for binary numbers. *Am. J. Phys.*, 58(10):1018, 1990.

[2] W. Metzler. The "mystery" of the quadratic Mandelbrot set. *Am. J. Phys.*, 62(9):813–814, 1994.

[3] R. Artzy. Dynamics of quadratic functions in cycle planes. *Jour. Geometry*, 44:26–32, 1992.

[4] D. G. Pavlov, Panchelyuga M. S., and Panchelyuga V. A. About shape of Julia set at zero parameter on double numbers plane. *Hypercomplex numbers y geometry and physics*, 6:146–151, 2009.

[5] D. G. Pavlov, Panchelyuga M. S., Malykhin V. A., and Panchelyuga V. A. On fractality of Mandelbrot and Julia sets on double-numbers plane. *Hypercomplex numbers y geometry and physics*, 6:135–145, 2009.

[6] A. Douady. *Julia sets and the Mandelbrot set.* Springer-Verlag, 1986.

[7] M. Fernández-Guasti and F. Zaldivar. A hyperbolic non distributive algebra in 1+2 dimensions. *Adv. Appl. Clifford Algebras*, 2013. in print.

[8] M. Fernández-Guasti. Alternative realization for the composition of relativistic velocities. In *Optics and Photonics 2011*, volume 8121 of *The nature of light: What are photons? IV*, page 812108–1–11. SPIE, 2011.

[9] M. Fernández-Guasti. Lagrange's identity obtained from product identity. *Int. Math. Forum*, 7(52):2555–2559, 2012.

[10] B. B. Mandelbrot. *Fractals and Chaos: The Mandelbrot Set and Beyond.* Springer, 2004.

[11] P. Willenius. Gestaltlupe. *https://github.com/trafassel/Gestaltlupe*, 2012.

[12] M. Fernandez-Guasti. scarexy2.gif. *http:/luz.izt.uam.mx/gallery2/v/sca/scare*, 2012.

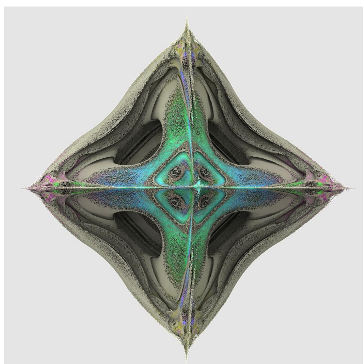

(a) 100

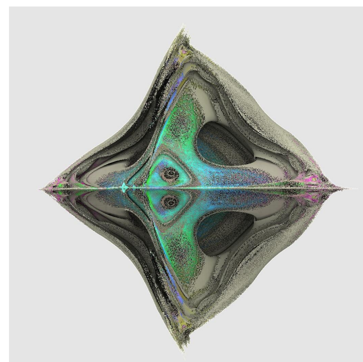

(b) 75

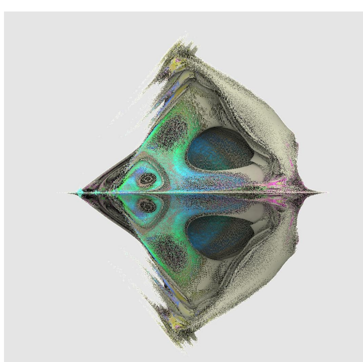

(c) 50

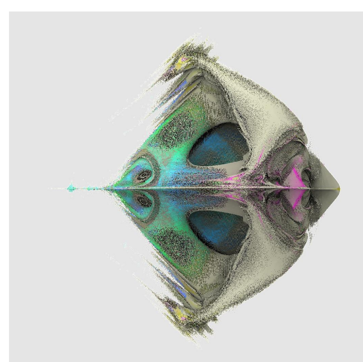

(d) 25

Figure 4: z angle

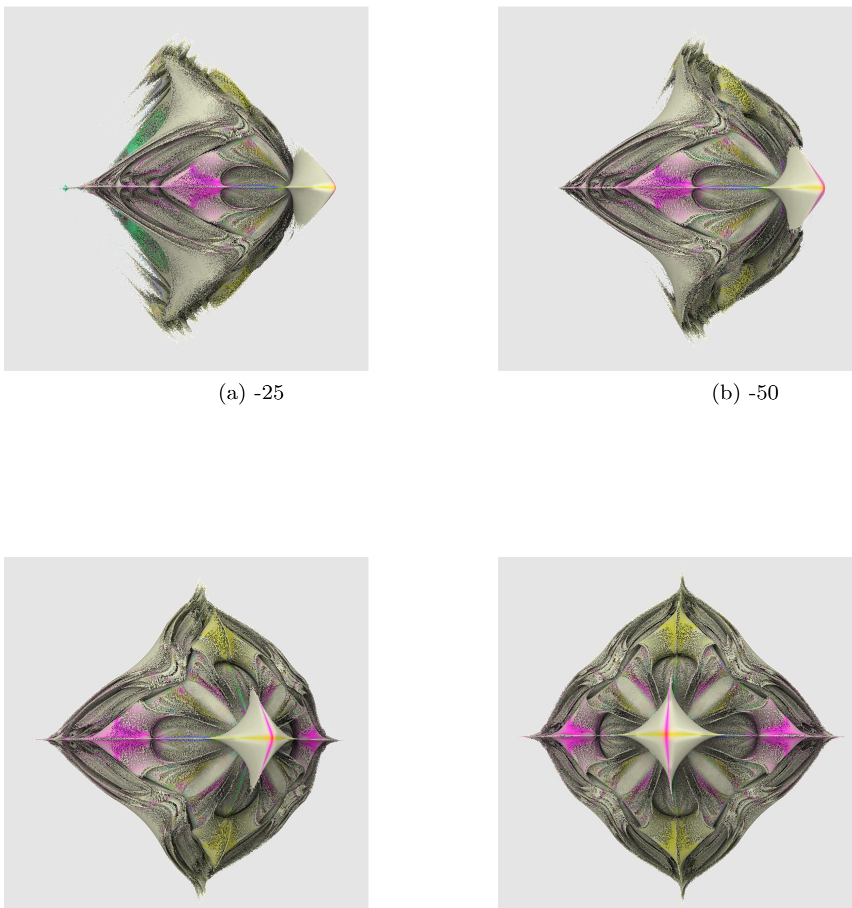

(a) -25 (b) -50

(c) -75 (d) -100

Figure 5: v

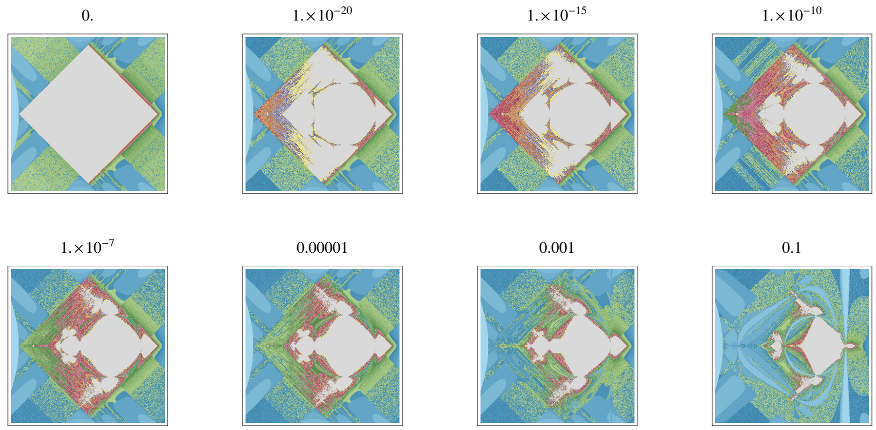

Figure 6: Slices for small y values in the $s, \hat{\mathbf{e}}_x$ plane of the bound quadratic iteration $\mathbf{c2i0}\mathbb{E}^2(s; x, y)$ set with constant second director component y between 0 and 0.1 labeled on the upper border of each frame.

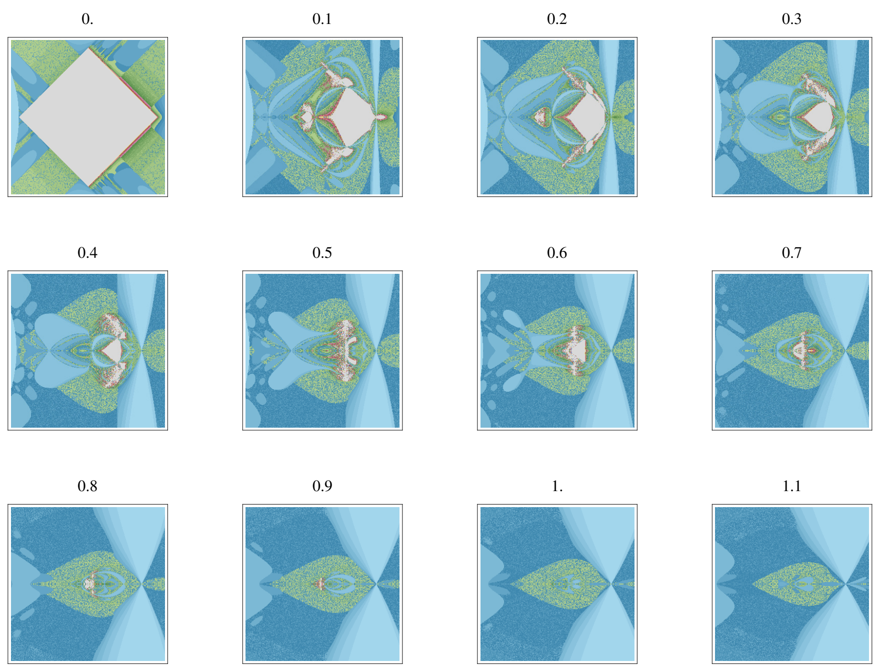

Figure 7: Slices of the bound quadratic iteration $\mathbf{c2i0}\mathbb{E}^2(s; x, y)$ set with y hyper-axis between 0 and 1.1 in 0.1 steps. The abscissa s is scanned in the ± 1.25 interval centered at -0.875 whereas the ordinate x is scanned in the same interval but centered at the origin.

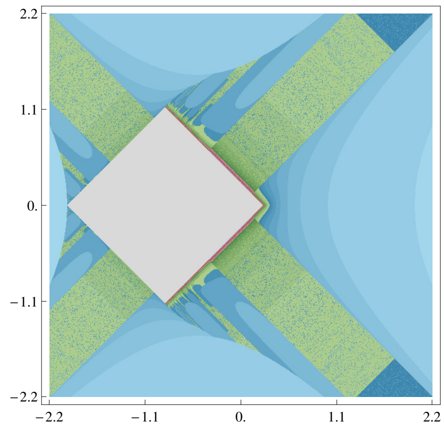

Figura 8: Bound set (in light gray) under quadratic iteration of hyperbolic numbers **c2i0**$\mathbb{H}$. Bounding condition is $a^2 - b^2 \leq 4$. (evaluation for each point is limited to 60 iterations).

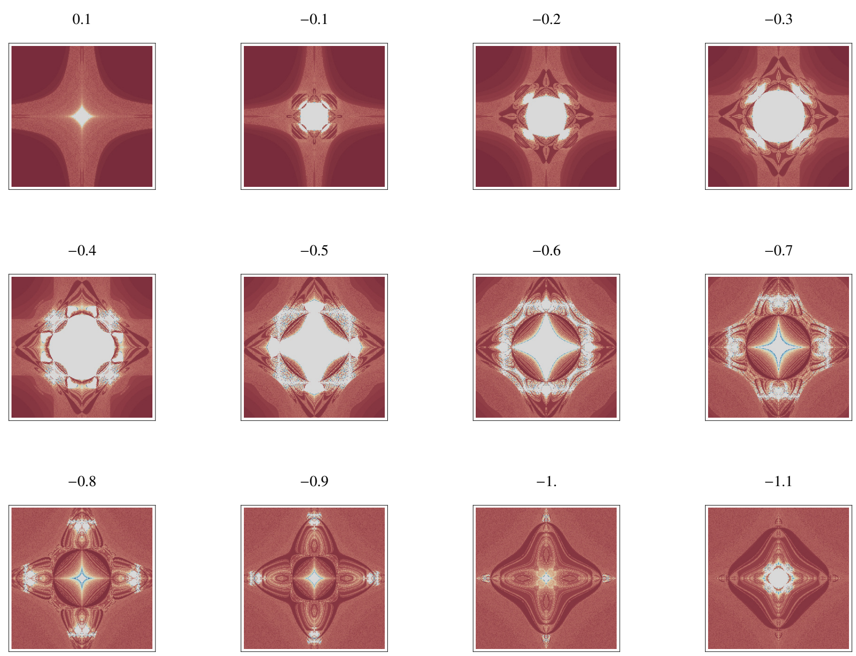

Figure 9: Slices of the **c2i0**$\mathbb{E}^2(s; x, y)$ sets (in light gray) shown at constant scalar component s. The x, y plane scans, where both axes represent hypercomplex components, span from -1 to 1 in both directions for all insets.

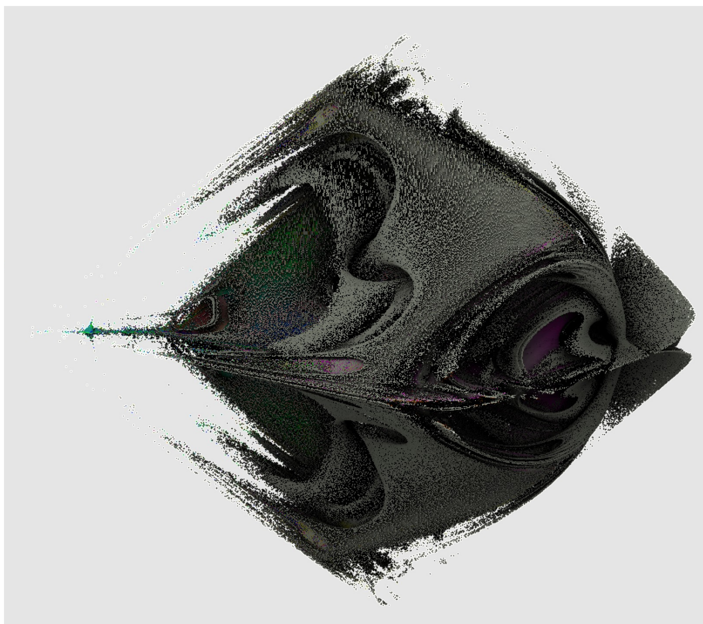

Figure 10: Three dimensional rendering of the $\mathbf{c2i0}\mathbb{E}^2(s; x, y)$ set produced with P. Willenius rendering program [11] . The bud on the far left (in light blue) is a self similar copy of the larger set. The straight lines leading to vertices, sharper on the upper part and in perspective comming out of the page, correspond to the squares obtained for the planes $x = 0$ and $y = 0$.